Full title

Advanced Glycation End Product 3 (AGE3) Suppresses the Mineralization of Mouse Stromal ST2 Cells and Human Mesenchymal Stem Cells by Increasing TGF-β Expression and Secretion

Authors' names and institutions

Masakazu Notsu, Toru Yamaguchi, Kyoko Okazaki, Ken-ichiro Tanaka, Noriko Ogawa, Ippei Kanazawa, and Toshitsugu Sugimoto

Internal Medicine 1, Shimane University Faculty of Medicine, Shimane, Japan

Running title

Effects of AGE-TGF-β signal on osteoblasts

Key words

Advanced Glycation End Products (AGEs), Bone quality deterioration, Osteoblast differentiation, TGF-β

Word Count

3996

Corresponding author's address, telephone and fax number, and email address

Address all correspondence and requests for reprints to: Toru Yamaguchi, Shimane University, 89-1, Enya-cho, Izumo, Shimane, 693-8501, Japan. Tel +81 853-20-2183, Fax +81 853-23-8650. E-mail: yamaguch@med.shimane-u.ac.jp

Disclosure Summary

M.N., T.Y., K.O., K.T., N.O., I.K., and T.S. have no potential conflicts of interest to declare.

Abstract

In diabetic patients, advanced glycation end products (AGEs) cause bone fragility because of deterioration of bone quality. We previously showed that AGEs suppressed the mineralization of mouse stromal ST2 cells. Transforming growth factor (TGF)-β is abundant in bone, and enhancement of its signal causes bone quality deterioration. However, whether TGF-β signaling is involved in the AGE-induced suppression of mineralization during the osteoblast lineage remains unknown. We therefore examined the roles of TGF-β in the AGE-induced suppression of mineralization of ST2 cells and human mesenchymal stem cells (hMSCs). AGE3 significantly (P<0.001) inhibited mineralization in both cell types, whereas transfection with siRNA for the receptor for AGEs (RAGE) significantly (P<0.05) recovered this process in ST2 cells. AGE3 increased (P<0.001) the expression of TGF-β mRNA and protein, which was partially antagonized by transfection with RAGE siRNA. Treatment with a TGF-β type I receptor kinase inhibitor, SD208, recovered AGE3-induced decreases in osterix (P<0.001) and osteocalcin (P<0.05) and antagonized the AGE3-induced increase in Runx2 mRNA expression in ST2 cells (P<0.001). Moreover, SD208 completely and dose-dependently rescued AGE3-induced suppression of mineralization in both cell types. In contrast, SD208 intensified AGE3-induced suppression of cell proliferation as well as AGE3-induced apoptosis in proliferating ST2 cells. These findings indicate that, after cells become confluent, AGE3 partially inhibits the differentiation and mineralization of osteoblastic cells by binding to RAGE and increasing TGF-β expression and secretion. They also suggest that TGF-β adversely affects bone quality not only in primary osteoporosis but also in diabetes-related bone disorder.

Introduction

Both diabetes mellitus (DM) and osteoporotic fractures are important healthcare problems, because they affect quality of life and increase morbidity and mortality (1). Several community-based studies and some national databases indicate that the incidence of type 2 DM (T2DM) has increased over the past three decades (2). In Japan, as many as 13 million patients are thought to have osteoporosis, and this number is increasing (3-5). Previous studies have shown that, compared with nondiabetic subjects, patients with T2DM have a 1.4- to 4.7-fold increased risk of fracture, although they have normal or slightly increased bone mineral density (BMD) (6-8). These findings suggest that fracture risk in T2DM is not reflected by BMD but is related to bone fragility independent of BMD. Several studies have suggested that the pathogenesis of diabetic osteoporosis is related to decreased osteoblastic bone formation rather than increased osteoclastic bone resorption (9,10).

Hyperglycemia in DM accelerates the formation of advanced glycation end products (AGEs), which result from a chain of chemical reactions in plasma or tissue that follow nonenzymatic Browning reactions between reducing sugars and free reactive amino groups of proteins(11,12). The cellular interactions of AGEs are mediated by the receptor for AGE (RAGE), which is a multiligand receptor belonging to the immunoglobulin superfamily and exerts biologic effects through binding to its ligands, including AGEs. Pentosidine is an AGE, and an increase in pentosidine cross-links in bone matrix is reported to impair bone mechanical properties in the absence of decreased BMD (13). Other studies have also shown a positive association between serum or urinary pentosidine levels and fracture risk in T2DM patients (14,15). Therefore, AGEs may act as causative factors for poor bone quality. In contrast, low serum levels of endogenous soluble RAGE, which has extensive neutralizing effects against various AGEs, are a risk factor for the vertebral fractures prevalent in T2DM patients (16). In an in vitro study, we found that AGE2 and AGE3 suppressed the mineralization of mouse stromal ST2 cells (17,18) by inhibiting the expression of osteoblastogenetic mRNAs such as those for osteocalcin (OCN) and osterix (OSX) (19,20). Moreover, these AGEs significantly suppressed cell growth and increased apoptotic cell death (19). However, the biologic substances that mediate these detrimental effects of AGEs on the osteoblast lineage remain unknown.

Transforming growth factor (TGF)-β is a multifunctional polypeptide that regulates a variety of cellular functions, including cell proliferation, differentiation, migration, and apoptosis under physiologic and pathologic conditions (21). TGF-β is sequestered at high levels in bone matrix and is a critical regulator of osteogenesis (22). TGF-β activates intracellular Smad3, which, in turn, binds Runx2 at the *runx2* and *OCN* promoters to

repress the transcription of genes required for osteoblast differentiation (23,24). Previous animal studies have shown that reducing TGF-β signaling leads to increases in functional parameters of bone quality such as bone stiffness, as evaluated by the three-point bending test (25-27). Moreover, another animal study has shown that inhibition of TGF-β type 1 receptor kinase has anabolic and anti-catabolic effects on bone by increasing both BMD and bone stiffness (28). These findings suggest that TGF-β signaling has detrimental effects on bone quality.

There is a documented association between AGE–TGF-β signaling and diabetic complications. In humans and in animal models, TGF-β mRNA and protein levels are significantly increased in the glomeruli and tubulointerstitium in diabetes (29-31), and administration of neutralizing anti-TGF-β antibodies to STZ-induced diabetic mice prevents glomerular hypertrophy (32). Moreover, AGEs stimulate TGF-β expression by mesangial cells (33,34). In addition, TGF-β levels are significantly higher in patients with diabetic neuropathy than in those without it (35). In an experiment using human peripheral nerve microvascular endothelial cells, AGEs induced basement membrane hypertrophy and disrupted the blood–nerve barrier by the action of autocrine TGF-β released by pericytes (36). In the retina, TGF-β is important in controlling the formation of new vessels, and TGF-β1 is upregulated in proliferative diabetic retinopathy (37). Matsumoto et al. (38) reported a relationship between glycoxidation and cytokine levels in the vitreous of eyes with diabetic retinopathy, and they suggested that elevated levels of pentosidine and TGF-β may play an important role in the development of diabetic retinopathy. Together, these findings suggest that AGEs can cause diabetic complications in the kidneys, nerves, and retina by increasing TGF-β levels. However, whether AGEs adversely affect osteoblastic mineralization and differentiation during diabetic bone disorder by enhancing TGF-β signals—as is seen in other complications of diabetes—is unknown.

Here, we addressed this issue by evaluating the role of TGF-β in the AGE3-induced suppression of osteoblastic differentiation and mineralization of ST2 cells and human mesenchymal stem cells (hMSCs). We found that AGE3 inhibited the differentiation and mineralization of these cells in part by binding to RAGE and increasing TGF-β expression and secretion.

Materials and methods

Materials

Cell culture medium and supplements were purchased from GIBCO-BRL (Rockville, MD).

Human recombinant BMP-2 was kindly provided by Astellas Pharmaceutical (Tokyo, Japan). All other chemicals were of the highest grade available commercially.

Cell culture

Mouse ST2 cells were purchased from the RIKEN Cell Bank (Tsukuba, Japan). They were cultured under 5% CO_2 at 37 °C in α-minimum essential medium (α-MEM; containing 5.5 mmol/L glucose) supplemented with 10% fetal bovine serum (FBS) and 1% penicillin–streptomycin (GIBCO-BRL); the culture medium was changed twice weekly. To induce osteoblastic differentiation, ST2 cells were cultured in α-MEM supplemented with 10% FBS, 1% penicillin–streptomycin, 5 mM β-glycerophosphate, 100 μg/mL ascorbic acid, and 100 ng/mL BMP-2 after reaching confluence. hMSCs were purchased from Lonza (Walkersville, MD) and cultured in MSC basal medium (Lonza). To induce osteoblastic differentiation, hMSCs were cultured in MSC basal medium supplemented with 1% penicillin–streptomycin, β-glycerophosphate, 100 μg/mL ascorbic acid, and dexamethasone (Lonza) after reaching confluence.

Preparation of AGEs

AGE–BSA was prepared as described previously (20). AGE3 was prepared by incubating 50 mg/mL BSA (Sigma, St. Louis, MO) with 0.1 M glycolaldehyde (Sigma) at 37 °C for 7 days under sterile conditions in 0.2 M sodium phosphate buffer (pH 7.4) containing 5 mM diethylenetriamine–pentaacetic acid. As a negative control, nonglycated BSA was incubated under the same conditions, except for the absence of glycolaldehyde. After the incubation period, low-molecular–weight reactants and aldehydes were removed by using a PD-10 column (GE Healthcare Bio-Sciences AB, Uppsala, Sweden) and dialyzing against phosphate-buffered saline (PBS).

Mineralization assay

The mineralization of ST2 cells and hMSCs was assessed in 6-well or 12-well plates by using von Kossa staining and Alizarin Red staining. Cells were stained with $AgNO_3$ and fixed with 2.5% NaS_2O_3 according to the von Kossa method to detect phosphate deposits in bone nodules (20,39). At the same time, duplicate plates were fixed with ice-cold 70% ethanol and stained with Alizarin Red to detect calcification. For quantification, cells stained with Alizarin Red were destained with ethylpyridinium chloride, the extracted stain

was transferred to a 96-well plate, and the absorbance at a wavelength of 550 nm was measured with a microplate reader, as previously described (20,39).

Quantification of secreted TGF-β1

The concentration of TGF-β1 in whole-cell lysates or culture medium was determined by using commercially available diagnostic kits (R&D Systems, Minneapolis, MN). In brief, samples were activated with 1 N HCl for 10 min at room temperature, followed by neutralization with 1.2 N NaOH in HEPES. Samples were added to the wells of microtiter plates, which were coated with a monoclonal anti-TGF-β1 antibody. After incubation of the sample for 2 h at room temperature, a horseradish-peroxidase–conjugated polyclonal antibody against TGF-β1 was added and the plates were incubated for another 2 h. The assay was developed with peroxidase substrate for 30 min at room temperature in the dark. Absorbance was measured at 450 nm, and a reference wavelength of 540 nm was used. Standard curves for TGF-β1 were prepared by using serial dilutions of exogenous TGF-β1.

Real-time PCR quantification of gene expression

SYBR Green chemistry was used to quantify the amounts of mRNAs for TGF-β and a housekeeping gene, 36B4, according to an optimized protocol (20,39,40). Total RNA was isolated by using Trizol reagent (Invitrogen, San Diego, CA) and further cleaned by two successive phenol–chloroform extractions. First-strand cDNA was synthesized by using an oligo-dT primer and a SuperScript-III cDNA synthesis kit (Invitrogen). Sense and antisense oligonucleotide primers were designed according to published cDNA sequences by using Primer Express (version 2.0.0, Applied Biosystems, Carlsbad, CA). The cDNA was amplified by using an ABI PRISM 7000 sequence detection system (Applied Biosystems Inc.). The cDNA-specific SYBR Green Mix was incorporated into the PCR buffer provided in the QuantiTect SYBR PCR kit to allow for quantitative detection of the PCR product in a 25-μL reaction volume. The temperature profile of the reaction was 60 °C for 2 min, followed by 95 °C for 15 min and 40 cycles of denaturation at 94 °C for 15 s and annealing and extension at 60 °C for 1 min. Primer sequences were as follows: TGF-β, 5′-TGAACCAAGGAGACGGAATACAGG-3′ and 5’-GCCATGAGGAGCAGGAAGGG-3′; OCN, 5′-TGCTTGTGAC-GAGCTATCAG-3′ and 5’-GAGGACAGGGAGGATCAAGT-3′; OSX, 5′-CCCTTCTCAAGCACCAATGG-3′ and 5′-AGGGTGGGTAGTCATTTGCATAG-3′; Runx2,

5′-AAGTGCGGTGCAAACTTTCT-3′ and 5′-TCTCGGTGGCTGGTAGTG A-3′; and 36B4, 5′-AAGCGCGTCCTGGCATTGTCT-3′ and 5′-CCGCAGGGGCAGCAGTGGT-3′.

RNA interference for RAGE

RNA interference was used to downregulate the expression of RAGE in ST2 cells. RAGE small interfering RNA (siRNA) and negative-control siRNA duplexes were designed and synthesized by Ambion (Austin, TX). For gene knockdown experiments, ST2 cells were seeded in 6-well plates and cultured at 37 °C for 48 h in α-MEM containing 10% FBS and antibiotics, followed by 24 h incubation in medium without antibiotics. Cells then were transfected with siRNAs (50 nM) by using Lipofectamine (Invitrogen, San Diego, CA) according to the manufacturer's instructions. After another 48 h of culture, cells were transferred to another plate containing fresh α-MEM supplemented with 10% FBS and antibiotics.

Evaluation of cell proliferation

ST2 cells ware seeded on 96-well plates at a density of 3000 cells/well and were incubated overnight in α-MEM containing 10% FBS and antibiotics. The next day, the cells were treated with either BSA (negative control) or AGE3. At the end of the experimental protocol, ST2 cells were labeled with bromodeoxyuridine (BrdU) for 2 h at 37 ºC. The ST2 cells then were fixed and denatured for 30 min at room temperature, followed by exposure to a peroxidase-conjugated anti-BrdU antibody (Roche Diagnotics, Indianapolis, IN) for 90 min at room temperature. The ST2 cells then were washed three times with PBS and incubated with a peroxidase substrate solution (Roche Diagnotics, Indianapolis, IN) at room temperature until the development of a noticeable color. The color change was quantified by using the absorption spectrometer to determine the amount of cell proliferation. An absorbance wavelength of 370 nm and reference wavelength of 492 nm were used.

Assessment of apoptotic cell death

ST2 cells ware seeded on 96-well plates at a density of 3000 cells/well and incubated overnight at 37 °C in α-MEM with 10% FBS and antibiotics. The next day, the cells were treated with either BSA (negative control) or AGE3. The cells then were lysed, and the DNA fragments in the supernatant were quantified in an ELISA (Cell Death Detection ELISA Plus, Roche Molecular Biochemicals, Indianapolis, IN) on day 3 after treatment.

Apoptosis was evaluated in differentiated ST2 cells and hMSCs. Cells were treated with either BSA or AGE3, as described earlier, on day 11 after reaching confluence. On day 14, the cells were lysed, and DNA fragments in the supernatant were analyzed by using an ELISA (Roche Molecular Biochemicals).

Statistical analysis

Results are expressed as means ± SEM. Differences between groups were evaluated by using one-way analysis of variance (ANOVA), followed by Fisher's protected least significant difference test. For all statistical tests, a value of $P < 0.05$ was considered to indicate a statistically significant difference.

Results

Effect of AGE3 on mineralization of ST2 cells and hMSCs

Treatment of ST2 cells with 200 μg/mL AGE3 for 14 and 21 days or of hMSCs with 200 μg/mL AGE3 for 14 days inhibited mineralization according to both von Kossa and Alizarin Red staining (Figures 1A and C). Alizarin red quantification analysis of ST2 cells and hMSCs showed that AGE3 significantly ($P < 0.001$) inhibited mineralization by 71% on experimental day 21 and 83% on day 14, respectively, relative to control values (Figure 1B and D) .

Effect of RAGE siRNA on AGE-suppressed mineralization in ST2 cells

AGEs are known ligands of RAGE, and we previously showed that AGE3 significantly increased RAGE mRNA expression in ST2 cells on days 2 and 3 after treatment (19,20). We therefore investigated whether transfection with RAGE siRNA recovered the mineralization suppressed by AGE3 in ST2 cells. RAGE siRNA transfection partially but significantly ($P < 0.05$) decreased the amount of RAGE mRNA (Figure 2A), and the mineralization of the transfected cells recovered by 17% ($P < 0.01$), as determined by Alizarin Red staining and quantification (Figure 2B). This result suggests that AGE3 suppresses the mineralization of ST2 cells in part by binding to RAGE.

Effects of AGE3 on expression of TGF-β mRNA and protein in ST2 cells and hMSCs

Next, we examined the effects of AGE3 on the expression of TGF-β mRNA and protein in ST2 cells and hMSCs. According to real-time PCR assays, AGE3 significantly ($P < 0.001$ all comparisons) increased the

expression of TGF-β mRNA in ST2 cells on days 3, 5, and 7 after treatment (Figure 3A). AGE3 also significantly increased TGF-β protein levels of ST2 supernatants on days 5 and 7 ($P < 0.01$) and whole-cell lysates on days 1 through 7 ($P < 0.001$), as measured with ELISAs (Figure 3B). In hMSCs, AGE3 significantly ($P < 0.001$) increased the levels of TGF-β protein in whole-cell lysates on days 1 through 7 (Figure 3B). Transfection of RAGE siRNA into ST2 cells decreased ($P < 0.05$) the AGE3-induced increase in TGF-β protein secretion by 24%, as determined by ELISA (Figure 4).

Effects of a TGF-β type I receptor kinase inhibitor on expression of OSX and OCN mRNAs in ST2 cells and on AGE-suppressed mineralization in ST2 cells and hMSCs

We previously showed that OSX and OCN mRNA levels in ST2 cells were suppressed by AGE3 (19). Here, we used real-time PCR assays to examine the effects of a TGF-β type I receptor kinase inhibitor, SD208, on these processes. Treatment with SD208 (2.5 μM) significantly ($P < 0.05$) recovered the expression of OSX and OCN mRNAs in ST2 cells on day 14 (Figure 5A and B, respectively). In contrast, treatment with SD208 significantly ($P < 0.001$) antagonized the AGE3-induced increase in Runx2 mRNA expression in ST2 cells on day 14 (Figure 5C). Moreover, Alizarin Red staining showed that treatment with SD208 (1 to 2.5 μM) significantly ($P < 0.001$) and dose-dependently recovered the AGE3-induced suppression of mineralization in ST2 cells and hMSCs (Figure 6A and B).

Effects of AGE3 and SD208 on proliferation and apoptosis of proliferating ST2 cells and on apoptosis of differentiating ST2 cells and hMSCs

We previously reported that AGE3 decreased cell growth and increased apoptosis in subconfluent ST2 cells (19). We therefore examined the effects of SD208 on the number and apoptosis of AGE3-treated ST2 cells to clarify the role of TGF-β signaling in proliferation of ST2 cells. Treatment with SD208 (2.5 μM) significantly ($P < 0.001$ both comparisons) intensified the AGE3-induced suppression of ST2 cell growth (Figure 7A), as well as their AGE3-induced apoptosis (Figure 7B). We also examined the effects of AGE3 or SD208 on the apoptosis of ST2 and hMSCs in the mature stages. The results showed that these agents did not affect the apoptosis of either cell type after they had reached confluence and began differentiation (that is, on days 11 through 14; data not shown).

Discussion

Here, we found that AGE3 suppresses mineralization of mouse stromal ST2 cells as well as hMSCs by increasing TGF-β expression and secretion (Figures 3, 5, 6). Treatment with a TGF-β type I receptor kinase inhibitor, SD208, recovered the AGE3-induced decreases in OSX and OCN and antagonized the AGE3-induced increase in Runx2 mRNA expression in ST2 cells (Figure 5). Moreover, SD208 completely and dose-dependently recovered the AGE3-induced suppression of mineralization in both cell types (Figure 6). These findings suggest that AGE3–TGF-β signaling has negative effects on, and impairs osteoblastic differentiation in, both cell types at the maturation stage. Accumulating evidence indicates that the TGF-β signal suppresses osteoblast differentiation in vitro (23,24,41,42). Alliston et al. (23) showed that the TGF-β–Smad3 signal repressed the expression of Runx2 and OCN mRNAs at 48 h and 6 days, respectively, and decreased mineralization at 10 days in osteoblastic cells treated with TGF-β. Kang et al. (24) showed that a controlled balance of histone acetylation and deacetylation at the OSE2 sequence of the OCN promoter regulates osteoblastic differentiation and that TGF-β induces and stabilizes HDAC4 and HDAC5, which modulate the repression of Runx2-mediated transcription of the OCN gene. Their results indicated that the interaction of TGF-β/Smad3 signaling with HDACs represses Runx2 and OCN function in differentiating osteoblasts (22). Maeda et al. (41) showed that the TGF-β type I receptor kinase inhibitor, SB431542, greatly enhanced the osteoblastic differentiation of mouse C2C12 cells. Takeuchi et al. (42) reported that treatment with SB431542 inhibited endogenous TGF-β and increased the formation of mineralized nodules. These authors demonstrated that inhibition of TGF-β released stromal cells from differentiation arrest due to multiple myeloma and facilitated the formation of terminally differentiated osteoblasts (40). Our findings that SD208-induced inhibition of TGF-β signaling increased the mineralization of ST2 cells and hMSCs agree with these previous results and suggest that AGEs augment these inhibitory effects of TGF-β on osteoblastic differentiation.

We found that the AGE3–TGF-β signal increased Runx2 mRNA expression in ST2 cells on day 14 after treatment with AGE3. Our preliminary experiments showed that AGE3 treatment did not affect Runx2 mRNA expression in the cells on day 7, indicating that Runx2 mRNA expression increased during the late stage of cell differentiation. Runx2 is known to have contradictory effects during the early, compared with late, stages of osteoblastic differentiation. During early differentiation, Runx2 directs multipotent mesenchymal cells to the osteoblast lineage and inhibits them from differentiating along the adipocyte and chondrocyte lineages. In contrast, after multipotent mesenchymal cells differentiate to preosteoblasts, Runx2 directs them toward

becoming immature osteoblasts but inhibits their further maturation and transition into osteocytes, keeping osteoblasts in an immature stage (43). Therefore, the suppression of OCN and OSX expression and the AGE3-associated enhancement of Runx2 expression at the late osteoblastic differentiation stage likely would act in concert to inhibit the differentiation of preosteoblasts to mineralizing mature osteoblasts and seems to be in accord with the AGE3-induced suppression of mineralization of ST2 cells and hMSCs.

In our study and previous ones, our AGE3 preparation inhibited the mineralization of osteoblastic MC3T3-E1 and ST2 cells as well as hMSCs (19,20). These effects were not toxic, because we previously showed that AGE3 prepared by the same method enhanced the calcification of rat vascular smooth muscle cells, in contrast to its effect on these osteoblastic cells (44). These findings suggest that the biologic activities of our AGE3 preparation are similar to those of endogenous AGEs in patients with DM, namely bone fragility and vascular calcification.

We found that siRNA-induced inhibition of RAGE recovered AGE3-induced suppression of mineralization (Figure 2) and antagonized AGE3-induced increases in TGF-β protein in ST2 cells (Figure 4). These results demonstrate that, by binding to RAGE, AGE3 at least contributed to the increased expression of TGF-β protein and suppressed mineralization of ST2 cells. AGEs have multiple receptors, including RAGE, CD36, lectin-like oxidized low-density lipoprotein receptor 1, macrophage scavenger receptors, and AGER1, 2, and 3 (45-50). The presence of multiple AGE receptors may explain why RAGE siRNA had only a partial effect on the cells in our study. We performed another experiments using a neutralizing antibody against human RAGE (R & D systems, Minneapolis, MN), which has approximately 10% cross-reactivity with recombinant mouse RAGE, and found that the antibody failed to recover mineralization suppressed by AGE3 in ST2 cells or hMSCs at the concentration range from 5 to 15μg/ml (data not shown). It might be because these antibody concentrations were not high enough to block the RAGE activities in the cells.

TGF-β exerts contradictory effects on bone cells depending on their maturation stage. In proliferating osteoblasts, TGF-β stimulates osteoblastic proliferation and the formation of periosteal woven bone when it is injected directly onto the periostea of the parietal bones of rats (51,52). Treatment of human osteoblast cells with TGF-β downregulates the expression of the Wnt antagonist sFRP-1 and prolongs the life of these cells (53). Other researchers have shown that TGF-β decreases TNF-α-induced apoptosis in murine osteoblasts (54). In addition, TGF-β prevents the osteoblastic apoptosis induced by skeletal unloading via PI3K–Akt signaling (55). In contrast, several studies in mature osteoblasts have shown that the TGF-β signal suppresses osteoblastic

differentiation in vitro, as mentioned earlier (23,24,41,42,56). Another study has shown that TGF-β added to confluent cultures inhibits the formation of bone nodules by reducing their number and total area (57). In our study, when ST2 cells were proliferating and subconfluent, SD208-induced inhibition of TGF-β signaling intensified AGE3-induced suppression of cell growth and AGE3-induced cell apoptosis (Figure 7). These results suggest that the TGF-β signal antagonizes the detrimental effects of AGE3 by increasing cell number and reducing apoptosis in proliferating ST2 cells. These findings contrast with those we obtained by using confluent cells, in which the TGF-β signal augmented the detrimental effects of AGE3 on osteoblast differentiation. Therefore, our results also indicate that TGF-β has biphasic and contradictory effects in ST2 cells, depending on their maturation stage. These findings suggest that we should consider the extent of cell maturation when we target TGF-β signals to treat diabetic osteoporosis. Animal studies using diabetic and nondiabetic wild-type and RAGE knockout mice are needed to demonstrate the role of TGF-β in diabetic bone loss and to ascertain the relevance of our findings in the clinical context.

A recent meta-analysis (7) showed that, compared with non-DM controls, T2DM patients had higher spine and hip BMD than did non-DM controls (z-scores = 0.41 and 0.27, respectively) but T1DM patients had lower spine and hip BMD (z-scores = –0.22 and –0.37, respectively). This discrepancy is partly because T2DM patients typically are obese and insulin resistant, whereas T1DM patients lack these features. Several studies have shown that body weight is positively correlated with BMD, probably because of mechanical stress, and that loss of body weight lowers BMD values (58-60). The increased levels of circulating insulin due to insulin resistance may exert anabolic actions on bone (61), and high BMD is a very consistent finding across a wide range of hyperinsulinemic states (62,63). However, clinical studies (64,65) have shown that serum OCN levels are lower in T2DM patients than in non-DM subjects and that serum OCN increases after glycemic control is achieved in diabetic patients. These findings indicate that T2DM patients still have diminished bone formation despite slightly increased BMD. Because here we examined the effects of AGEs on osteoblastic differentiation in the absence of mechanical stress or high insulin levels, our study design likely reflects the conditions of typical T1DM and of T2DM without obesity or insulin resistance.

Our study had several limitations. We did not examine whether AGE receptors other than RAGE or other components of TGF-β and the RAGE signaling pathway were involved in the inhibition of osteoblastic differentiation of ST2 cells and hMSCs. In addition, we did not examine the signals that mediated

AGE3-induced suppression of osteoblast proliferation and stimulation of apoptosis, nor the crosstalk between AGE signals and TGF-β signals.

In conclusion, we found that AGE3 inhibited the differentiation and mineralization of osteoblastic ST2 cells and hMSCs by binding to RAGE and increasing TGF-β expression and secretion after the cells reached confluence. These findings suggest that TGF-β causes a deterioration in bone quality, not only during primary osteoporosis but also during diabetes-related bone disorder, and that TGF-β adversely affects not only kidney, retina, and nerves, but also the bone, as part of diabetic complications.

Acknowledgement

This work was supported in part by Grant-in-Aid No. 25460898 (to T.Y.) from the Ministry of Science, Education and Culture of Japan.

Reference

1. **Johnell O, Kanis JA, Oden A, Sernbo I, Redlund-Johnell I, Petterson C, De Laet C, Jonsson B** 2004 Mortality after osteoporotic fractures. Osteoporos Int 15(1):38-42.
2. **Fox CS, Pencina MJ, Meigs JB, Vasan RS, Levitzky YS, D'Agostino RB, Sr.** 2006 Trends in the incidence of type 2 diabetes mellitus from the 1970s to the 1990s: the Framingham Heart Study. Circulation 113(25):2914-2918.
3. **Yoshimura N, Muraki S, Oka H, Kawaguchi H, Nakamura K, Akune T** 2010 Cohort profile: research on Osteoarthritis/Osteoporosis Against Disability study. Int J Epidemiol 39(4):988-995.
4. **Orimo H, Yaegashi Y, Onoda T, Fukushima Y, Hosoi T, Sakata K** 2009 Hip fracture incidence in Japan: estimates of new patients in 2007 and 20-year trends. Arch Osteoporos 4(1-2):71-77.
5. **Yoshimura N, Muraki S, Oka H, Mabuchi A, En-Yo Y, Yoshida M, Saika A, Yoshida H, Suzuki T, Yamamoto S, Ishibashi H, Kawaguchi H, Nakamura K, Akune T** 2009 Prevalence of knee osteoarthritis, lumbar spondylosis, and osteoporosis in Japanese men and women: the research on osteoarthritis/osteoporosis against disability study. J Bone Miner Metab 27(5):620-628.
6. **Schwartz AV, Sellmeyer DE, Ensrud KE, Cauley JA, Tabor HK, Schreiner PJ, Jamal SA, Black DM, Cummings SR** 2001 Older women with diabetes have an increased risk of fracture: a prospective study. J Clin Endocrinol Metab 86(1):32-38.

7. **Vestergaard P** 2007 Discrepancies in bone mineral density and fracture risk in patients with type 1 and type 2 diabetes--a meta-analysis. Osteoporos Int 18(4):427-444.

8. **Yamamoto M, Yamaguchi T, Yamauchi M, Kaji H, Sugimoto T** 2009 Diabetic patients have an increased risk of vertebral fractures independent of BMD or diabetic complications. J Bone Miner Res 24(4):702-709.

9. **Bouillon R, Bex M, Van Herck E, Laureys J, Dooms L, Lesaffre E, Ravussin E** 1995 Influence of age, sex, and insulin on osteoblast function: osteoblast dysfunction in diabetes mellitus. J Clin Endocrinol Metab 80(4):1194-1202.

10. **Kanazawa I, Yamaguchi T, Yamamoto M, Yamauchi M, Yano S, Sugimoto T** 2009 Serum osteocalcin/bone-specific alkaline phosphatase ratio is a predictor for the presence of vertebral fractures in men with type 2 diabetes. Calcif Tissue Int 85(3):228-234.

11. **Singh R, Barden A, Mori T, Beilin L** 2001 Advanced glycation end-products: a review. Diabetologia 44(2):129-146.

12. **Pongor S, Ulrich PC, Bencsath FA, Cerami A** 1984 Aging of proteins: isolation and identification of a fluorescent chromophore from the reaction of polypeptides with glucose. Proceedings of the National Academy of Sciences of the United States of America 81(9):2684-2688.

13. **Saito M, Fujii K, Mori Y, Marumo K** 2006 Role of collagen enzymatic and glycation induced cross-links as a determinant of bone quality in spontaneously diabetic WBN/Kob rats. Osteoporos Int 17(10):1514-1523.

14. **Yamamoto M, Yamaguchi T, Yamauchi M, Yano S, Sugimoto T** 2008 Serum pentosidine levels are positively associated with the presence of vertebral fractures in postmenopausal women with type 2 diabetes. J Clin Endocrinol Metab 93(3):1013-1019.

15. **Schwartz AV, Garnero P, Hillier TA, Sellmeyer DE, Strotmeyer ES, Feingold KR, Resnick HE, Tylavsky FA, Black DM** 2009 Cummings SR, Harris TB, Bauer DC. Pentosidine and increased fracture risk in older adults with type 2 diabetes. J Clin Endocrinol Metab 94(7):2380-2386.

16. **Yamamoto M, Yamaguchi T, Yamauchi M, Sugimoto T** 2009 Low serum level of the endogenous secretory receptor for advanced glycation end products (esRAGE) is a risk factor for prevalent vertebral fractures independent of bone mineral density in patients with type 2 diabetes. Diabetes Care 32(12):2263-2268.

17. **Otsuka E, Yamaguchi A, Hirose S, Hagiwara H** 1999 Characterization of osteoblastic differentiation of stromal cell line ST2 that is induced by ascorbic acid. Am J Physiol 277(1 Pt 1):C132-138.

18. **Yamaguchi A, Ishizuya T, Kintou N, Wada Y, Katagiri T, Wozney JM, Rosen V, Yoshiki S** 1996 Effects of BMP-2, BMP-4, and BMP-6 on osteoblastic differentiation of bone marrow-derived stromal cell lines, ST2 and MC3T3-G2/PA6. Biochem Biophys Res Commun 220(2):366-371.

19. **Okazaki K, Yamaguchi T, Tanaka K, Notsu M, Ogawa N, Yano S, Sugimoto T** 2012 Advanced glycation end products (AGEs), but not high glucose, inhibit the osteoblastic differentiation of mouse stromal ST2 cells through the suppression of osterix expression, and inhibit cell growth and increasing cell apoptosis. Calcif Tissue Int 91(4):286-296.

20. **Ogawa N, Yamaguchi T, Yano S, Yamauchi M, Yamamoto M, Sugimoto T** 2007 The combination of high glucose and advanced glycation end-products (AGEs) inhibits the mineralization of osteoblastic MC3T3-E1 cells through glucose-induced increase in the receptor for AGEs. Horm Metab Res 39(12):871-875.

21. **Massague J, Blain SW, Lo RS** 2000 TGFbeta signaling in growth control, cancer, and heritable disorders. Cell 103(2):295-309.

22. **Janssens K, ten Dijke P, Janssens S, Van Hul W** 2005 Transforming growth factor-beta1 to the bone. Endocr Rev 26(6):743-774.

23. **Alliston T, Choy L, Ducy P, Karsenty G, Derynck R** 2001 TGF-beta-induced repression of CBFA1 by Smad3 decreases cbfa1 and osteocalcin expression and inhibits osteoblast differentiation. EMBO J 20(9):2254-2272.

24. **Kang JS, Alliston T, Delston R, Derynck R** 2005 Repression of Runx2 function by TGF-beta through recruitment of class II histone deacetylases by Smad3. EMBO J 24(14):2543-2555.

25. **Balooch G, Balooch M, Nalla RK, Schilling S, Filvaroff EH, Marshall GW, Marshall SJ, Ritchie RO, Derynck R, Alliston T** 2005 TGF-beta regulates the mechanical properties and composition of bone matrix. Proceedings of the National Academy of Sciences of the United States of America 102(52):18813-18818.

26. **Chang JL, Brauer DS, Johnson J, Chen CG, Akil O, Balooch G, Humphrey MB, Chin EN, Porter AE, Butcher K, Ritchie RO, Schneider RA, Lalwani A, Derynck R, Marshall GW, Marshall SJ, Lustig L, Alliston T** 2010 Tissue-specific calibration of extracellular matrix material

properties by transforming growth factor-beta and Runx2 in bone is required for hearing. EMBO Rep 11(10):765-771.

27. **Edwards JR, Nyman JS, Lwin ST, Moore MM, Esparza J, O'Quinn EC, Hart AJ, Biswas S, Patil CA, Lonning S, Mahadevan-Jansen A, Mundy GR** 2010 Inhibition of TGF-beta signaling by 1D11 antibody treatment increases bone mass and quality in vivo. J Bone Miner Res 25(11):2419-2426.

28. **Mohammad KS, Chen CG, Balooch G, Stebbins E, McKenna CR, Davis H, Niewolna M, Peng XH, Nguyen DH, Ionova-Martin SS, Bracey JW, Hogue WR, Wong DH, Ritchie RO, Suva LJ, Derynck R, Guise TA, Alliston T** 2009 Pharmacologic inhibition of the TGF-beta type I receptor kinase has anabolic and anti-catabolic effects on bone. PLoS One 4(4):e5275.

29. **Yamamoto T, Nakamura T, Noble NA, Ruoslahti E, Border WA** 1993 Expression of transforming growth factor beta is elevated in human and experimental diabetic nephropathy. Proceedings of the National Academy of Sciences of the United States of America 90(5):1814-1818.

30. **Iwano M, Kubo A, Nishino T, Sato H, Nishioka H, Akai Y, Kurioka H, Fujii Y, Kanauchi M, Shiiki H, Dohi K** 1996 Quantification of glomerular TGF-beta 1 mRNA in patients with diabetes mellitus. Kidney Int 49(4):1120-1126.

31. **Pankewycz OG, Guan JX, Bolton WK, Gomez A, Benedict JF** 1994 Renal TGF-beta regulation in spontaneously diabetic NOD mice with correlations in mesangial cells. Kidney Int 46(3):748-758.

32. **Sharma K, Jin Y, Guo J, Ziyadeh FN** 1996 Neutralization of TGF-beta by anti-TGF-beta antibody attenuates kidney hypertrophy and the enhanced extracellular matrix gene expression in STZ-induced diabetic mice. Diabetes 45(4):522-530.

33. **Throckmorton DC, Brogden AP, Min B, Rasmussen H, Kashgarian M** 1995 PDGF and TGF-beta mediate collagen production by mesangial cells exposed to advanced glycosylation end products. Kidney Int 48(1):111-117.

34. **Ziyadeh FN, Han DC, Cohen JA, Guo J, Cohen MP** 1998 Glycated albumin stimulates fibronectin gene expression in glomerular mesangial cells: involvement of the transforming growth factor-beta system. Kidney Int 53(3):631-638.

35. **Ybarra J, Pou JM, Romeo JH, Merce J, Jurado J** 2010 Transforming growth factor beta 1 as a biomarker of diabetic peripheral neuropathy: cross-sectional study. J Diabetes Complications

24(5):306-312.

36. **Shimizu F, Sano Y, Haruki H, Kanda T** 2011 Advanced glycation end-products induce basement membrane hypertrophy in endoneurial microvessels and disrupt the blood-nerve barrier by stimulating the release of TGF-beta and vascular endothelial growth factor (VEGF) by pericytes. Diabetologia 54(6):1517-1526.

37. **Pfeiffer A, Spranger J, Meyer-Schwickerath R, Schatz H** 1997 Growth factor alterations in advanced diabetic retinopathy: a possible role of blood retina barrier breakdown. Diabetes 46 Suppl 2:S26-30.

38. **Matsumoto Y, Takahashi M, Ogata M** 2002 Relationship between glycoxidation and cytokines in the vitreous of eyes with diabetic retinopathy. Jpn J Ophthalmol 46(4):406-412.

39. **Kanazawa I, Yamaguchi T, Yano S, Yamauchi M, Sugimoto T** 2010 Fasudil hydrochloride induces osteoblastic differentiation of stromal cell lines, C3H10T1/2 and ST2, via bone morphogenetic protein-2 expression. Endocr J 57(5):415-421.

40. **Livak KJ, Schmittgen TD** 2001 Analysis of relative gene expression data using real-time quantitative PCR and the 2(-Delta Delta C(T)) Method. Methods 25(4):402-408.

41. **Maeda S, Hayashi M, Komiya S, Imamura T, Miyazono K** 2004 Endogenous TGF-beta signaling suppresses maturation of osteoblastic mesenchymal cells. EMBO J 23(3):552-563.

42. **Takeuchi K, Abe M, Hiasa M, Oda A, Amou H, Kido S, Harada T, Tanaka O, Miki H, Nakamura S, Nakano A, Kagawa K, Yata K, Ozaki S, Matsumoto T** 2010 Tgf-Beta inhibition restores terminal osteoblast differentiation to suppress myeloma growth. PLoS One 5(3):e9870.

43. **Komori T** 2006 Regulation of osteoblast differentiation by transcription factors. J Cell Biochem 99(5):1233-1239.

44. **Tada Y, Yano S, Yamaguchi T, Okazaki K, Ogawa N, Morita M, Sugimoto T** 2013 Advanced glycation end products-induced vascular calcification is mediated by oxidative stress: functional roles of NAD(P)H-oxidase. Horm Metab Res 45(4):267-272.

45. **Suzuki H, Kurihara Y, Takeya M, Kamada N, Kataoka M, Jishage K, Ueda O, Sakaguchi H, Higashi T, Suzuki T, Takashima Y, Kawabe Y, Cynshi O, Wada Y, Honda M, Kurihara H, Aburatani H, Doi T, Matsumoto A, Azuma S, Noda T, Toyoda Y, Itakura H, Yazaki Y, Kodama T, et al** 1997 A role for macrophage scavenger receptors in atherosclerosis and susceptibility to infection.

Nature 386(6622):292-296.

46. Araki N, Higashi T, Mori T, Shibayama R, Kawabe Y, Kodama T, Takahashi K, Shichiri M, Horiuchi S 1995 Macrophage scavenger receptor mediates the endocytic uptake and degradation of advanced glycation end products of the Maillard reaction. Eur J Biochem 230(2):408-415.

47. Ramasamy R, Yan SF, Schmidt AM 2011 Receptor for AGE (RAGE): signaling mechanisms in the pathogenesis of diabetes and its complications. Ann N Y Acad Sci 1243:88-102.

48. Ohgami N, Nagai R, Ikemoto M, Arai H, Kuniyasu A, Horiuchi S, Nakayama H 2001 Cd36, a member of the class b scavenger receptor family, as a receptor for advanced glycation end products. J Biol Chem 276(5):3195-3202.

49. Rudijanto A 2007 The expression and down stream effect of lectin like-oxidized low density lipoprotein 1 (LOX-1) in hyperglycemic state. Acta Med Indones 39(1):36-43.

50. Lai KN, Leung JC, Chan LY, Li FF, Tang SC, Lam MF, Tse KC, Yip TP, Chan TM, Wieslander A, Vlassara H 2004 Differential expression of receptors for advanced glycation end-products in peritoneal mesothelial cells exposed to glucose degradation products. Clin Exp Immunol 138(3):466-475.

51. Noda M, Camilliere JJ 1989 In vivo stimulation of bone formation by transforming growth factor-beta. Endocrinology 124(6):2991-2994.

52. Fujimoto R, Tanizawa T, Nishida S, Yamamoto N, Soshi S, Endo N, Takahashi HE 1999 Local effects of transforming growth factor-beta1 on rat calvaria: changes depending on the dose and the injection site. J Bone Miner Metab 17(1):11-17.

53. Bodine PV, Billiard J, Moran RA, Ponce-de-Leon H, McLarney S, Mangine A, Scrimo MJ, Bhat RA, Stauffer B, Green J, Stein GS, Lian JB, Komm BS 2005 The Wnt antagonist secreted frizzled-related protein-1 controls osteoblast and osteocyte apoptosis. J Cell Biochem 96(6):1212-1230.

54. Chua CC, Chua BH, Chen Z, Landy C, Hamdy RC 2002 TGF-beta1 inhibits multiple caspases induced by TNF-alpha in murine osteoblastic MC3T3-E1 cells. Biochim Biophys Acta 1593(1):1-8.

55. Dufour C, Holy X, Marie PJ 2008 Transforming growth factor-beta prevents osteoblast apoptosis induced by skeletal unloading via PI3K/Akt, Bcl-2, and phospho-Bad signaling. Am J Physiol Endocrinol Metab 294(4):E794-801.

56. Borton AJ, Frederick JP, Datto MB, Wang XF, Weinstein RS 2001 The loss of Smad3 results in a

lower rate of bone formation and osteopenia through dysregulation of osteoblast differentiation and apoptosis. J Bone Miner Res 16(10):1754-1764.

57. **Harris SE, Bonewald LF, Harris MA, Sabatini M, Dallas S, Feng JQ, Ghosh-Choudhury N, Wozney J, Mundy GR** 1994 Effects of transforming growth factor beta on bone nodule formation and expression of bone morphogenetic protein 2, osteocalcin, osteopontin, alkaline phosphatase, and type I collagen mRNA in long-term cultures of fetal rat calvarial osteoblasts. J Bone Miner Res 9(6):855-863.

58. **Edelstein SL, Barrett-Connor E** 1993 Relation between body size and bone mineral density in elderly men and women. Am J Epidemiol 138(3):160-169.

59. **Hannan MT, Felson DT, Anderson JJ** 1992 Bone mineral density in elderly men and women: results from the Framingham osteoporosis study. J Bone Miner Res 7(5):547-553.

60. **Nguyen TV, Sambrook PN, Eisman JA** 1998 Bone loss, physical activity, and weight change in elderly women: the Dubbo Osteoporosis Epidemiology Study. J Bone Miner Res 13(9):1458-1467.

61. **Reid IR** 2002 Relationships among body mass, its components, and bone. Bone 31:547-555.

62. **Abrahamsen B, Rohold A, Henriksen JE, Beck-Nielsen H** 2000 Correlations between insulin sensitivity and bone mineral density in non-diabetic men. Diabet Med 17:124-129.

63. **Reid IR, Evans MC, Cooper GJ, Ames RW, Stapleton J** 1993 Circulating insulin levels are related to bone density in normal postmenopausal women. Am J Physiol 265:E655-E659.

64. **Kanazawa I, Yamaguchi T, Yamauchi M, Yamamoto M, Kurioka S, Yano S, Sugimoto T** 2009 Adiponectin is associated with changes in bone markers during glycemic control in type 2 diabetes mellitus. J Clin Endocrinol Metab 94(8):3031-3037.

65. **Okazaki R, Totsuka Y, Hamano K, Ajima M, Miura M, Hirota Y, Hata K, Fukumoto S, Matsumoto T** 1997 Metabolic improvement of poorly controlled noninsulin-dependent diabetes mellitus decreases bone turnover. J Clin Endocrinol Metab 82(9):2915-2920.

Figure legends

Fig. 1 Effects of AGE3 on mineralization of ST2 cells and hMSCs.

Bovine serum albumin (BSA; control; 200 μg/mL) or AGE3 (200 μg/mL) was added after the cells reached confluence. (A) Alizarin Red and von Kossa staining of cultured ST2 cells on days 7, 14, and 21 after treatment with BSA or AGE3. (B) Quantification of Alizarin Red staining of the ST2 cells in each treatment

group. (C) Alizarin Red and von Kossa staining of cultured hMSCs on day 14 after treatment with BSA or AGE3. (D) Quantification of Alizarin Red staining of hMSCs in each treatment group.

***$P < 0.001$ compared with control. The results shown are representative of 3 independent experiments and are expressed as means ± SEM of fold increase relative to control (BSA) values (n = 6).

Fig. 2 Efficiency of knockdown of RAGE and effects of RAGE siRNA transfection in mineralization of ST2 cells suppressed by AGE3.

(A) Effect of siRNA on RAGE mRNA expression in ST2 cells. ST cells were transfected with siRNAs (50nM) by using Lipofectamine. Total RNA was collected on day 3 and RAGE mRNA was measured by real-time PCR. (B) Alizarin red staining was performed on day 7 after Negative control or RAGE siRNA transfection. Control BSA and AGE3 were added after the cells reached confluence. Plate view of Alizarin red staining in cultured ST2 cells with 200μg/mL of either control BSA or AGE3 for 14 days. (C) Quantification of Alizarin red staining of the cells with each treatment. *$p < 0.05$, **$p < 0.01$ and ***$p < 0.001$ compared to control.

Fig. 3 Effects of AGE3 on TGF-β mRNA (A) and protein expressions (B) in ST2 cells and hMSCs.

(A) Effects of AGE3 on TGF-β mRNA expressions in ST2 cells. Two hundred μg/mL of either control BSA or AGE3 were added after the cells reached confluence. Total RNA was collected on days 1, 3, 5 and 7, and TGF-β mRNA was measured by real-time PCR. Results are expressed as the mean ± SEM fold increase over control values (N = 10). *$p < 0.05$ and ***$p < 0.001$ compared to control on the same day. (B) Effects of AGE3 on TGF-β protein expressions in ST2 cells and hMSCs. Two hundred μg/mL of either control BSA or AGE3 were added after the cells reached confluence. Supernatants or whole cell lysates were collected on days 1, 3, 5 and 7. Quantification of TGF-β protein on days 1, 3, 5 and 7 was performed by ELISA. Results are expressed as the mean ± SEM (n = 6). **$p < 0.01$ and ***$p < 0.001$ compared to control on the same day.

Fig. 4 Effects of RAGE siRNA transfection on TGF-β protein expressions increased by AGE3 in ST2 cells.

Two hundred μg/mL of either control BSA or AGE3 were added after the cells reached confluence. Total RNA was collected on day 7 after RAGE siRNA transfection. Real-time PCR was performed as described

568 in Materials and Methods. *p ＜ 0.05 and ***p ＜ 0.001 compared to negative control siRNA.

569

570 Fig. 5 Effects of a TGF-β type I receptor kinase inhibitor on OSX（A）, OCN（B） and Runx2（C）mRNA
571 expressions affected by AGE3 in ST2 cells.

572 Two hundred μg/mL of either control BSA or AGE3 with or without SD208 (2.5 mM), a TGF-β
573 receptor kinase inhibitor, were added after the cells reached confluence. Total RNA was collected on day 14,
574 and OSX, OCN and Runx2 mRNA expressions were measured by real-time PCR. Results are expressed as the
575 mean ± SEM fold increase over control values (n = 6). *p ＜ 0.05, **p ＜ 0.01, and ***p ＜ 0.001
576 compared to levels of mRNA expressions treated with AGE3 alone.

577

578 Fig. 6 Effect of a TGF-β receptor type I kinase inhibitor in mineralization of ST2 cells (A) and hMSCs (B)
579 suppressed by AGE3.

580 Two hundred μg/mL of either control BSA or AGE3 were added after the cells reached confluence.
581 SD208 (1.0 or 2.5 mM) was added with AGE3 on the same time. Plate view of Alizarin red staining in cultured
582 ST2 cells and hMSCs for 14 days. Quantification of Alizarin red staining of the cells was performed with each
583 treatment. Results are expressed as the mean ± SEM fold increase over control values (n = 6). ***p ＜ 0.001
584 compared to Alizarin red quantity treated with AGE3 alone.

585

586 Fig. 7 Effects of a TGF-β receptor type I kinase inhibitor on the cell proliferation (A) and apoptosis (B) of ST2
587 cells.

588 (A) Effects of AGE3 with or without SD208 on the cell proliferation of ST2 cells. The cells were
589 seeded on 96-well plates at a density of 3000 cells/well, and were incubated overnight. On the next day, the cells
590 were treated with 200μg/mL of either control BSA or AGE3 in the presence or absence of 2.5 mM SD208 for 3
591 days. Cell proliferation was evaluated by BrdU on day 3. ***p ＜ 0.001 compared to AGE3 alone. (B)
592 Effects of AGE3 with or without SD208 on the apoptotic cell death of ST2 cells. The cells were seeded on
593 96-well plates at a density of 3000 cells/well and were incubated overnight. On the next day, the cells were
594 treated with 200μg/mL of either control BSA or AGE3 in the presence or absence of 2.5 mM SD208 for 3 days.
595 The apoptotic cell death was analyzed in an ELISA for DNA fragments by an absorbance at 405 nm. *p ＜
596 0.05 and ***p ＜ 0.001 compared to control BSA.

597

Fig. 1

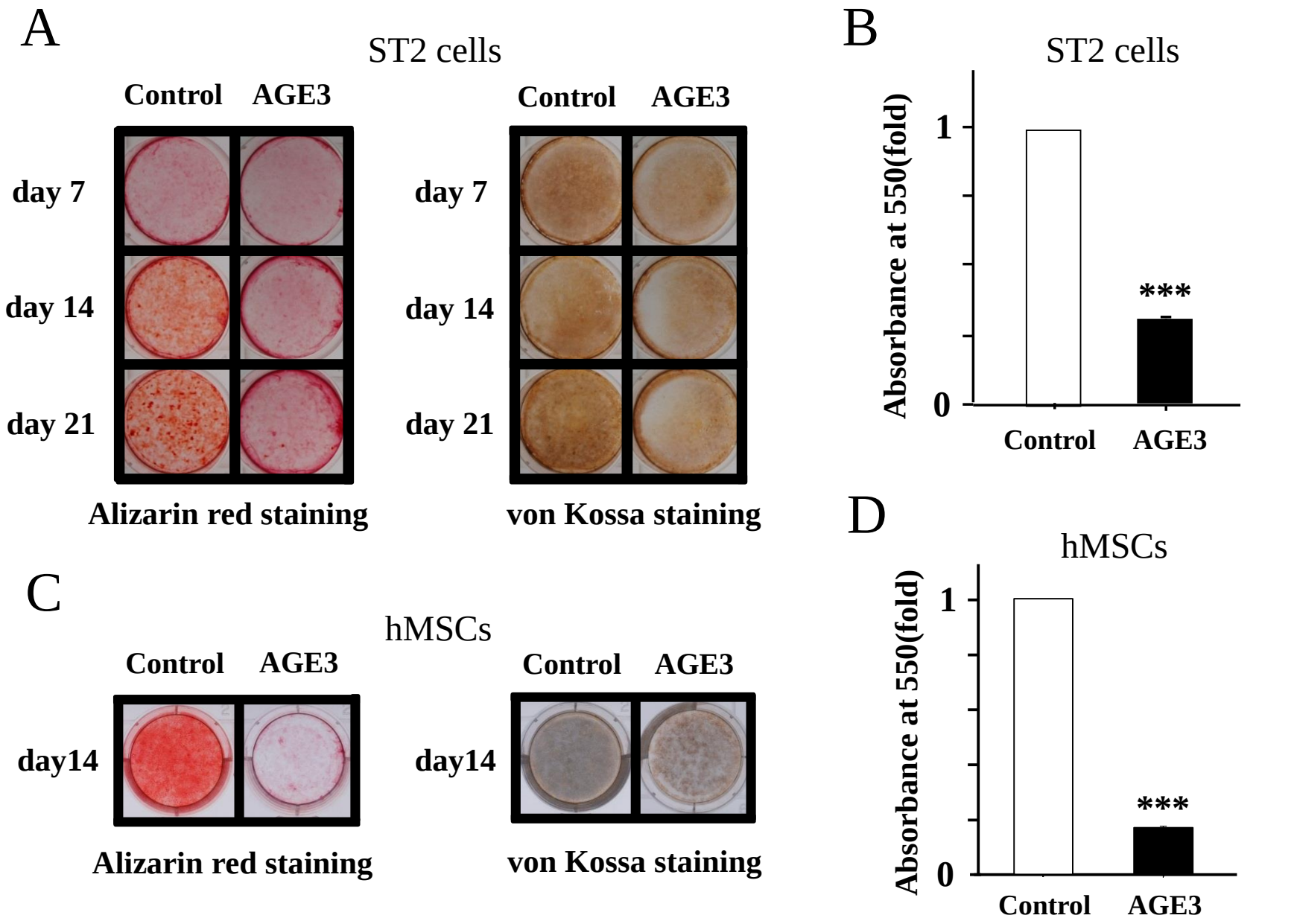
A
ST2 cells
Control
AGE3
Control
AGE3
day 7
day 14
day 21
day 7
day 14
day 21
Alizarin red staining
von Kossa staining
B
ST2 cells
Absorbance at 550(fold)
1
0
***
Control
AGE3
C
hMSCs
Control
AGE3
Control
AGE3
day14
day14
Alizarin red staining
von Kossa staining
D
hMSCs
Absorbance at 550(fold)
1
0
***
Control
AGE3

Fig. 2

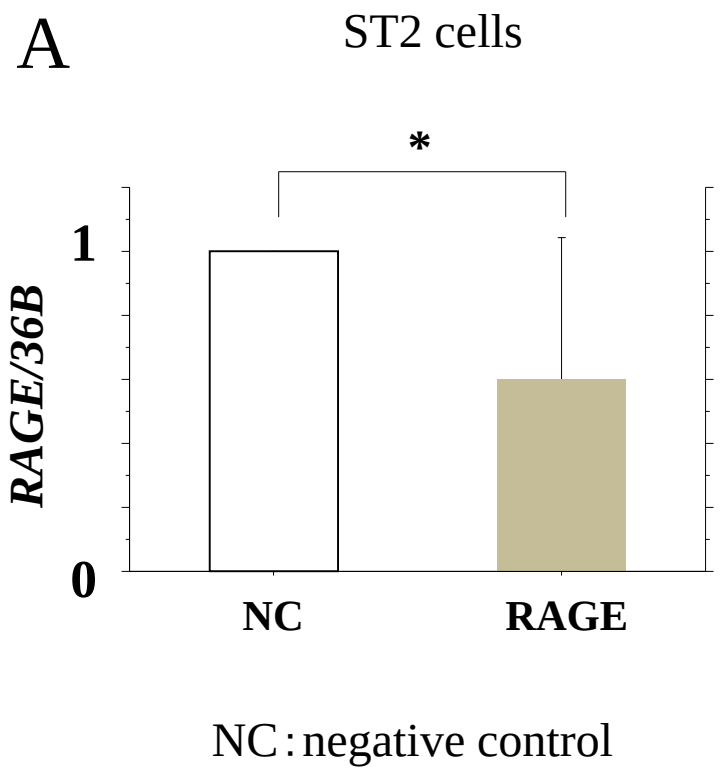

NC : negative control

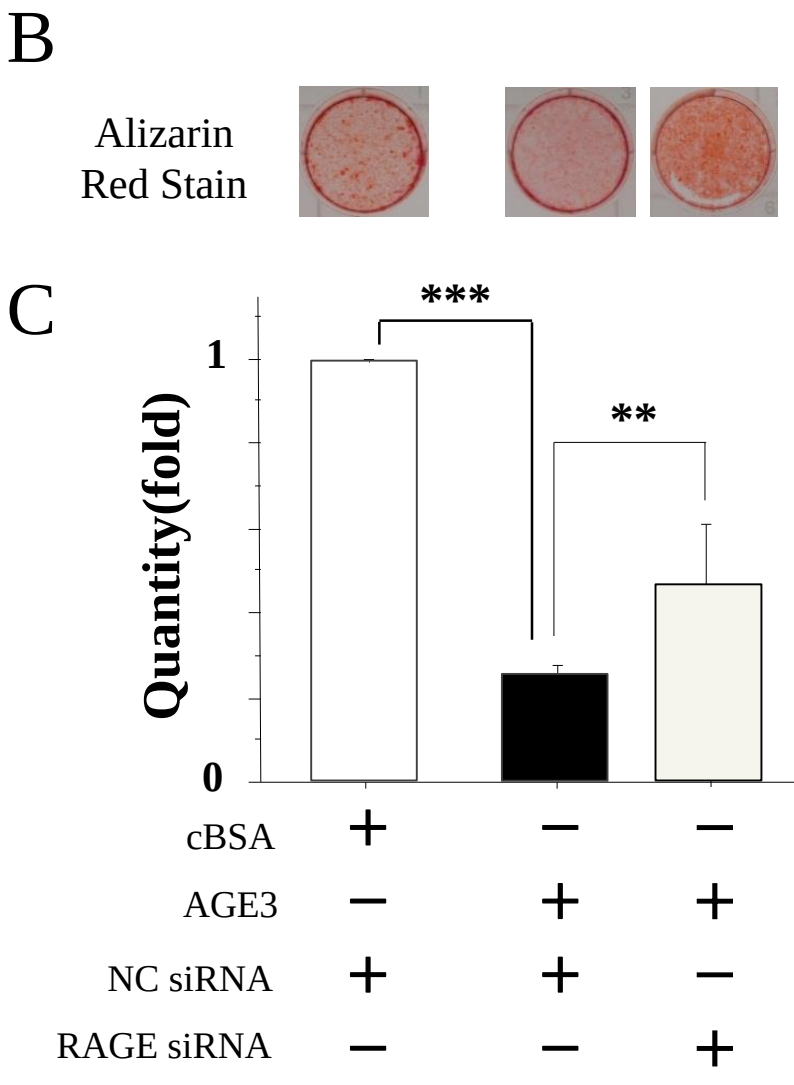

Fig. 3A

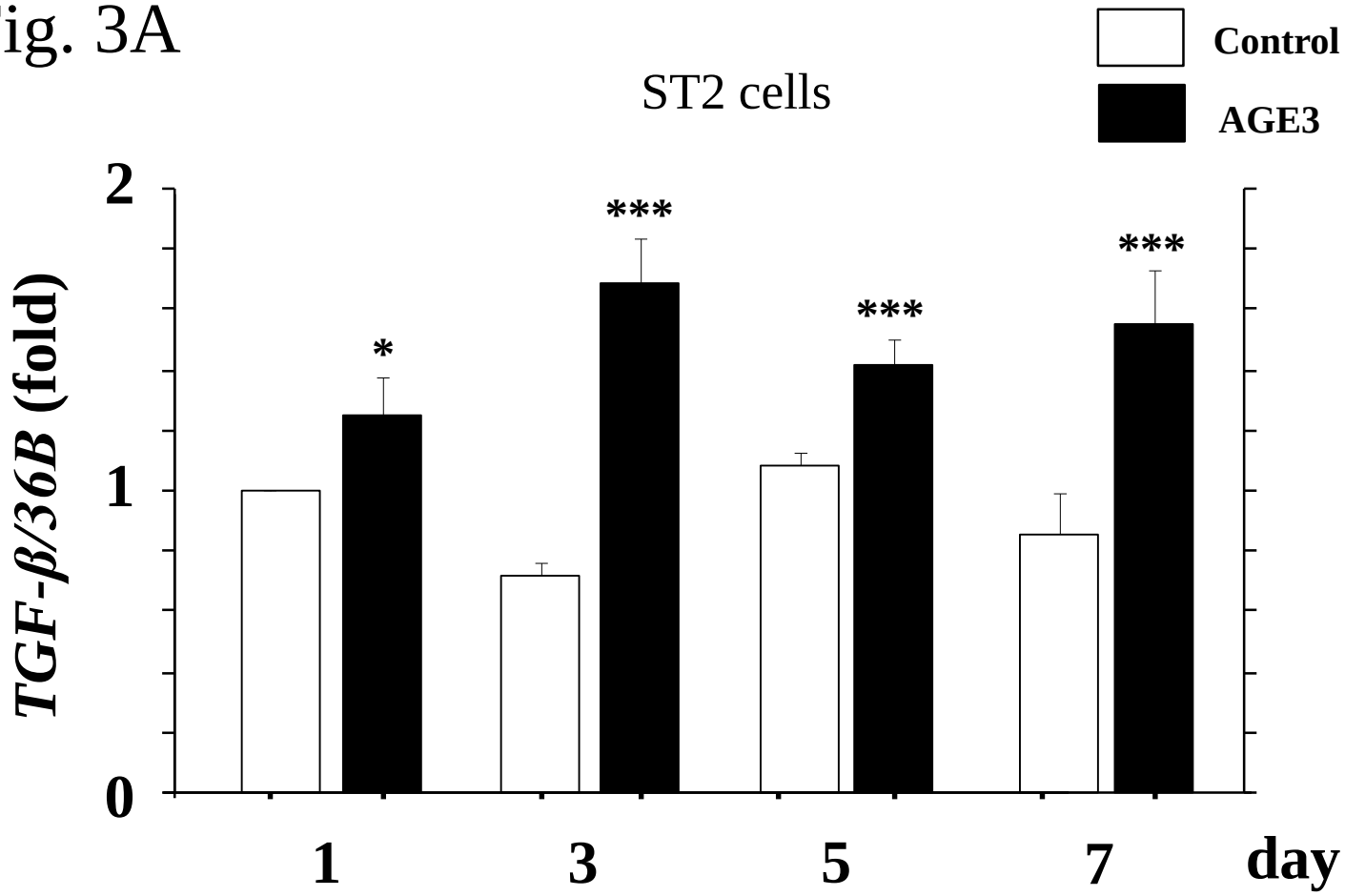

Fig.3B

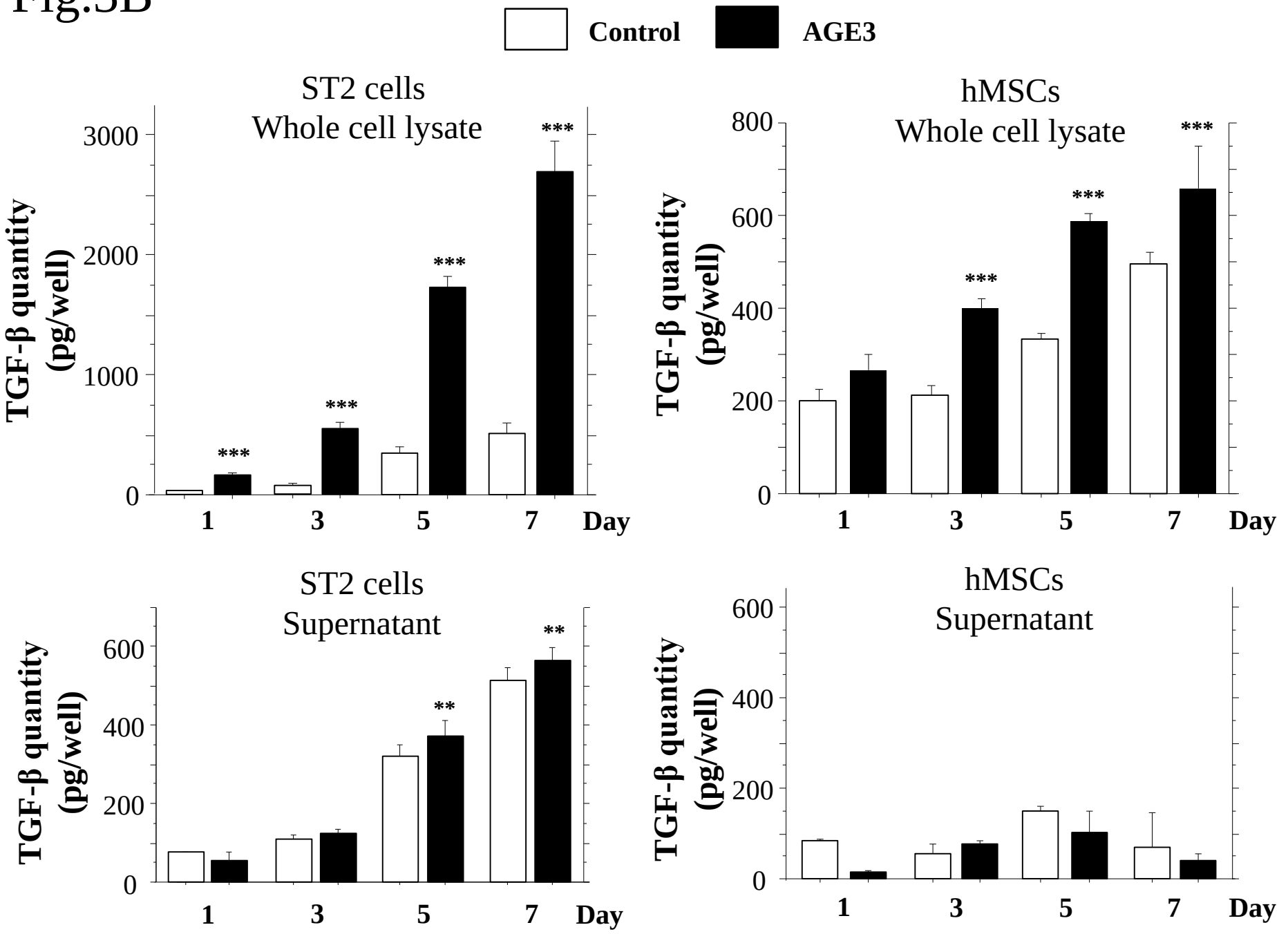
Control
AGE3
ST2 cells
Whole cell lysate
TGF-β quantity (pg/well)
3000
2000
1000
0
***
1
3
5
7
Day
hMSCs
Whole cell lysate
800
600
400
200
0
ST2 cells
Supernatant
**
hMSCs
Supernatant

Fig. 4

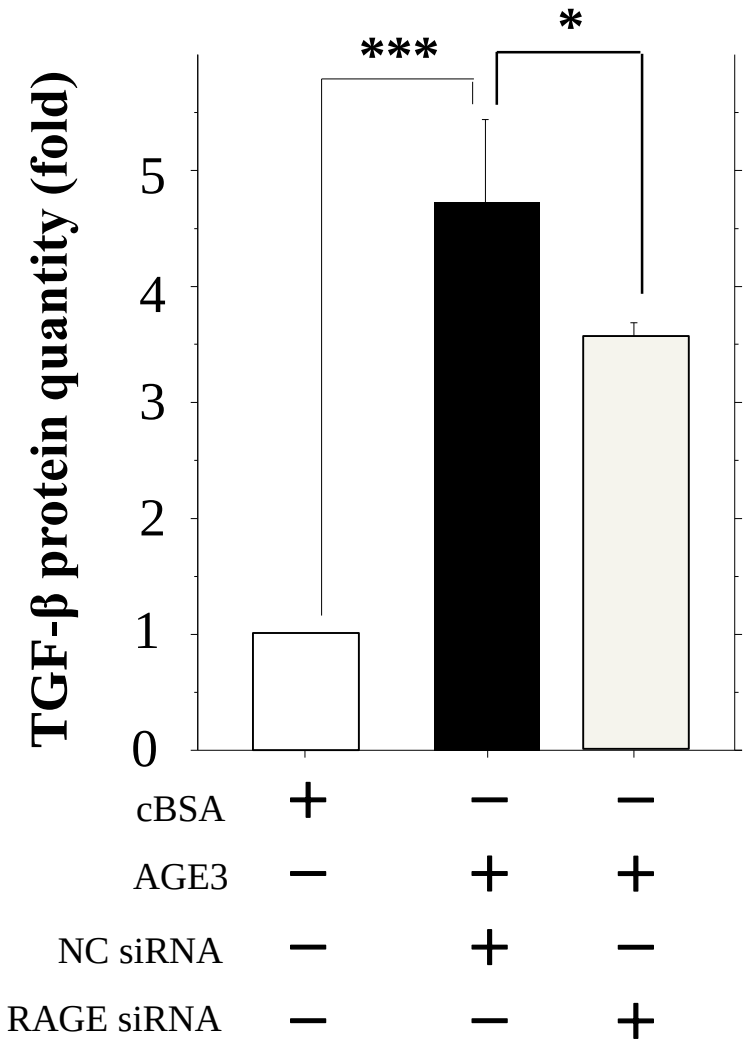
***
*
TGF-β protein quantity (fold)
0
1
2
3
4
5
cBSA + − −
AGE3 − + +
NC siRNA − + −
RAGE siRNA − − +

Fig. 5

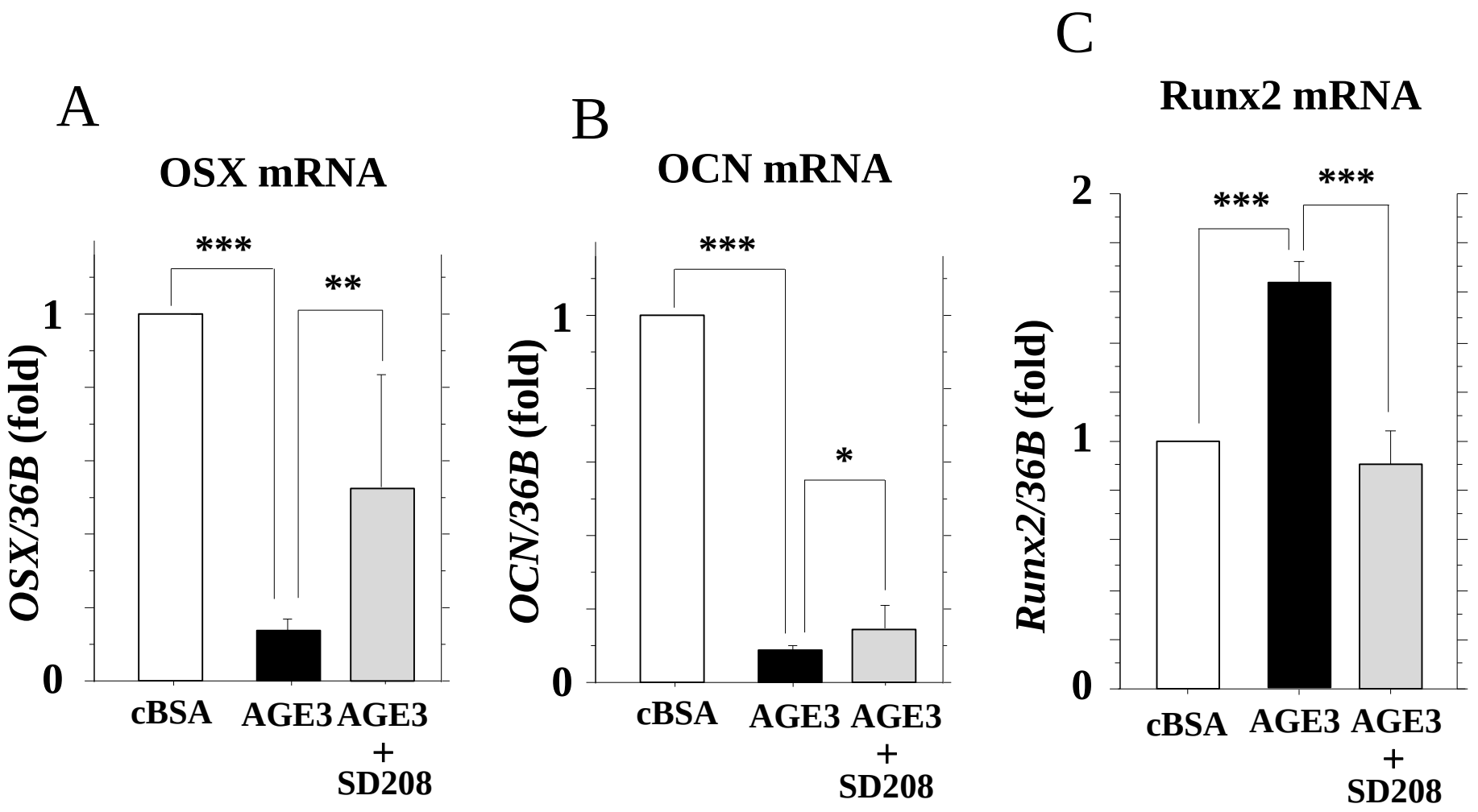
A
OSX mRNA
OSX/36B (fold)
1
0
***
**
cBSA
AGE3
AGE3 + SD208
B
OCN mRNA
OCN/36B (fold)
1
0
***
*
cBSA
AGE3
AGE3 + SD208
C
Runx2 mRNA
Runx2/36B (fold)
2
1
0
***
***
cBSA
AGE3
AGE3 + SD208

Fig. 6

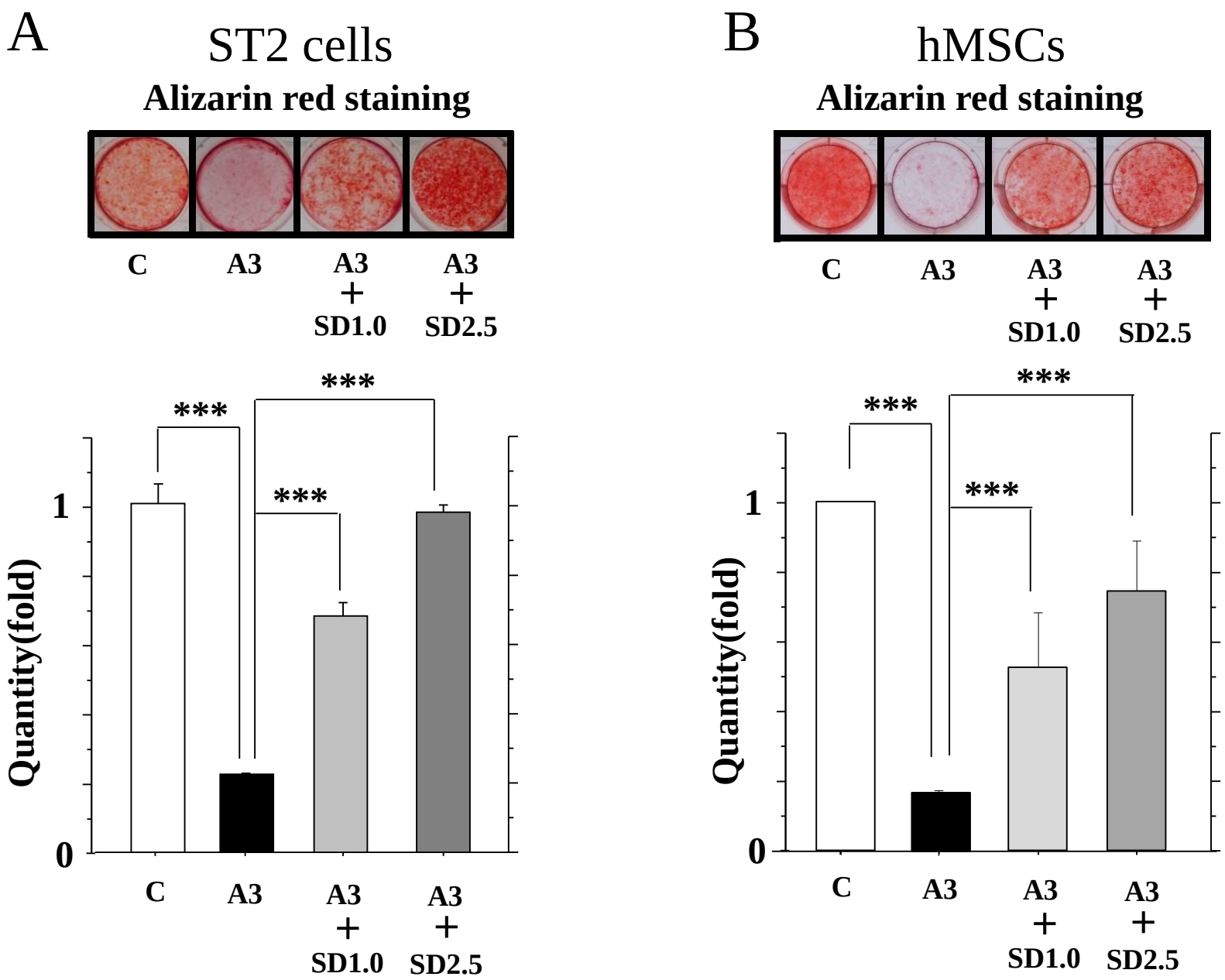
A
ST2 cells
Alizarin red staining
C
A3
A3 + SD1.0
A3 + SD2.5
***
***
***
Quantity(fold)
1
0
B
hMSCs
Alizarin red staining
C
A3
A3 + SD1.0
A3 + SD2.5
***
***
***
Quantity(fold)
1
0

Fig. 7

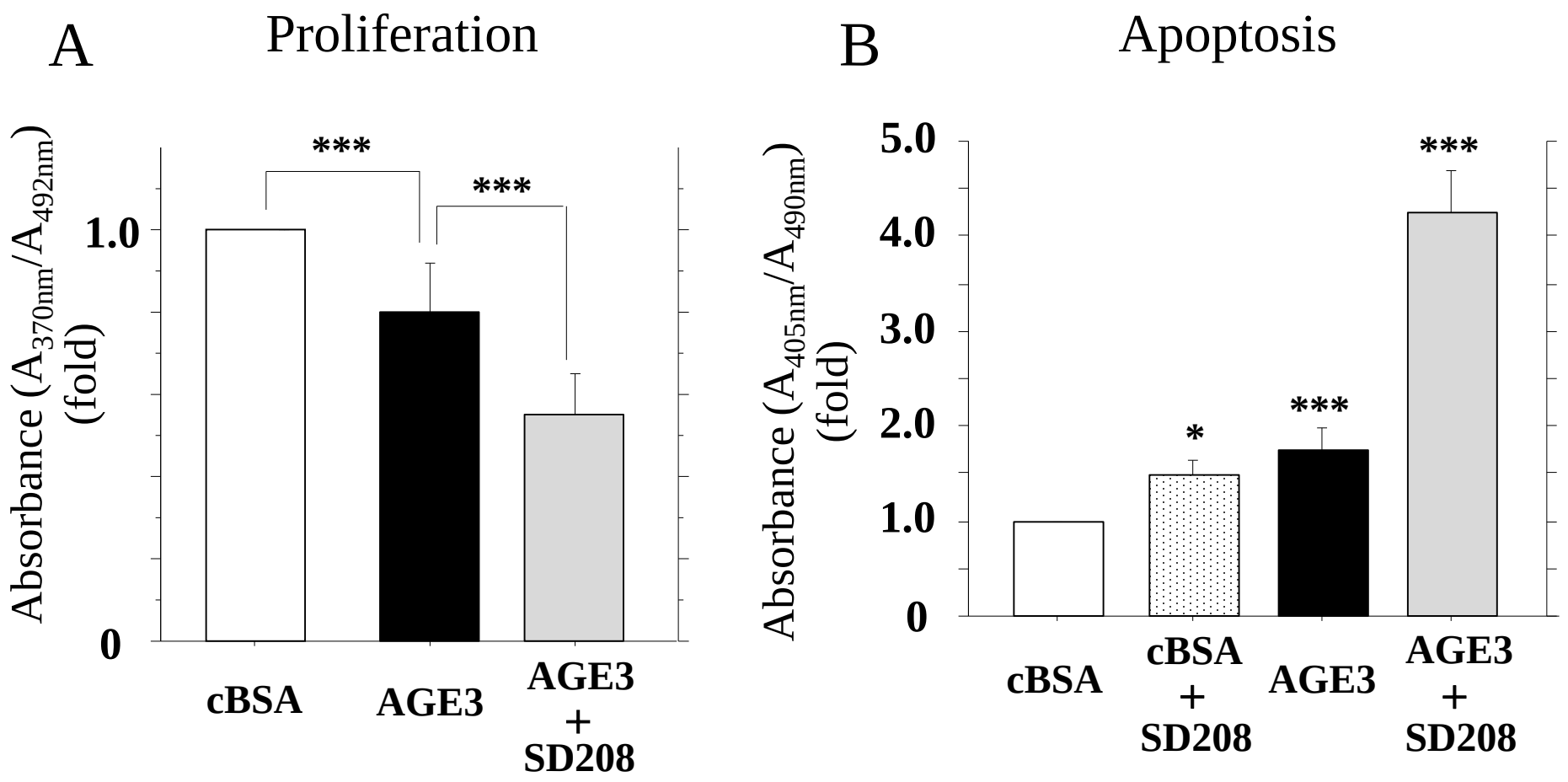
A
Proliferation
Absorbance (A_{370nm}/A_{492nm}) (fold)
1.0
0
***
***
cBSA
AGE3
AGE3 + SD208
B
Apoptosis
Absorbance (A_{405nm}/A_{490nm}) (fold)
5.0
4.0
3.0
2.0
1.0
0
*
***
***
cBSA
cBSA + SD208
AGE3
AGE3 + SD208